



**HAL**  
open science

# Kinetics and capacity of phosphorus extraction from solid residues obtained from wet air oxidation of sewage sludge

Cristian Barca, Mathieu Martino, Pierre Hennebert, Nicolas Roche

► **To cite this version:**

Cristian Barca, Mathieu Martino, Pierre Hennebert, Nicolas Roche. Kinetics and capacity of phosphorus extraction from solid residues obtained from wet air oxidation of sewage sludge. Waste Management, 2019, 89, pp.275-283. 10.1016/j.wasman.2019.04.024 . hal-02118222

**HAL Id: hal-02118222**

**<https://hal.science/hal-02118222>**

Submitted on 22 Oct 2021

**HAL** is a multi-disciplinary open access archive for the deposit and dissemination of scientific research documents, whether they are published or not. The documents may come from teaching and research institutions in France or abroad, or from public or private research centers.

L'archive ouverte pluridisciplinaire **HAL**, est destinée au dépôt et à la diffusion de documents scientifiques de niveau recherche, publiés ou non, émanant des établissements d'enseignement et de recherche français ou étrangers, des laboratoires publics ou privés.



Distributed under a Creative Commons Attribution - NonCommercial 4.0 International License

1 **Kinetics and capacity of phosphorus extraction from solid residues**  
2 **obtained from wet air oxidation of sewage sludge**

3 Cristian Barca<sup>1,\*</sup>, Mathieu Martino<sup>1</sup>, Pierre Hennebert<sup>2</sup>, Nicolas Roche<sup>3</sup>

4 <sup>1</sup> Aix-Marseille Univ., CNRS, Centrale Marseille, M2P2 UMR 7340, 13451 Marseille,  
5 France

6 <sup>2</sup> INERIS ARDEVIE, BP 2, F-60550 Verneuil-en-Halatte, France

7 <sup>3</sup> Aix Marseille Univ, CNRS, IRD, INRA, Coll France, CEREGE, BP 80, 13545 Aix-  
8 en-Provence, France

9 \*corresponding author: [cristian.barca@univ-amu.fr](mailto:cristian.barca@univ-amu.fr)

10

11 **Abstract**

12 Solid residues from thermal treatments of sewage sludge (SS) represent a valuable  
13 source of phosphorus (P) for the fertilizer production. This study aims at evaluating the  
14 P recovery potential from solid residues obtained from wet air oxidation of SS under  
15 subcritical water conditions (WAO residues). A series of P extraction experiments was  
16 performed by acidic and alkaline leaching at different liquid to solid ratios. Hot  
17 chemical extractions and P fractionations were also carried out to characterize the  
18 chemical composition of the WAO residues. The main objectives of this work were to  
19 determine the best operating conditions for P extraction, and to describe and understand  
20 the kinetics and the main mechanisms leading to P release. The results obtained in this  
21 study indicate that 1 M citric acid and 1 M HCl at the liquid to solid ratio of 10 L/kg can  
22 extract 61% and 65% of the total P content after 2 h of contact time at room

23 temperature, thus giving P extraction capacities of 81 and 86 g P/kg WAO residues,  
24 respectively. The analysis of kinetic data indicates that P extraction with 1 M HCl is  
25 faster, but 1 M citric acid can give higher P extraction efficiencies at the equilibrium.  
26 The molar ratios of Ca to P of the leachates suggest that P extraction from WAO  
27 residues was primarily due to the dissolution of a mixture of various Ca-P complexes.  
28 **Keywords:** phosphorus recovery; sewage sludge; wet air oxidation residue; acidic  
29 leaching; kinetic model.

30

## 31 **1 Introduction**

32 Nowadays, industrial production of chemical fertilizers strongly depends on non-  
33 renewable phosphorus (P) sources such as natural deposits of phosphate minerals (*e.g.*  
34 apatite rocks), and the evaluation of alternative renewable resources for fertilizer  
35 production today represents a critical research topic for ensuring the future global food  
36 security (Cordell et al., 2011; Desmidt et al., 2015). Indeed, the demand of chemical  
37 fertilizers for food production is rising rapidly due to the increase in world population,  
38 and recent prospective studies have indicated that a peak of P extraction from apatite  
39 rocks will occur at around 2020, and then P is likely to become a critical resource by  
40 2050 (Cordell et al., 2011; Desmidt et al., 2015; Sørensen et al., 2015). There is  
41 therefore an urgent need to identify alternative renewable P sources for the fertilizer  
42 production.

43 Currently, there is a general consensus among researchers that P recovery from  
44 wastewater may represent a promising way to overcome the shortage of natural  
45 resources (Ciešlik and Konieczka, 2017; Cordell et al., 2011; Herzel et al., 2016; Melia

46 et al., 2017). Moreover, the removal of P from wastewater can significantly reduce the  
47 supply of this nutrient to sensitive aquatic ecosystems, thus reducing the risk of  
48 eutrophication. The results of Cordell et al. (2011) indicate that more than 25% of the P  
49 demand in 2100 can be met by recovering P from agricultural and municipal  
50 wastewater. In particular, sewage sludge (SS) from municipal wastewater treatment  
51 plants (WWTPs) shows one of the most interesting potentials for P recovery, due to  
52 their relatively high and constant content in P (Melia et al., 2017).

53 A large number of processes have been proposed by researchers and practitioners to  
54 recover P from SS, such as the direct reuse as fertilizers in the fields, the precipitation of  
55 struvite and hydroxyapatite from the sludge leachates, and the extraction of P from the  
56 solid residues (*e.g.* char and ashes) that are obtained after thermal treatments of SS  
57 (Cieślik and Konieczka, 2017). Among these different techniques, P recovery from char  
58 and ashes presents several advantages compared to the other recovery techniques, as  
59 thermal treatments of SS usually provide: (i) the destruction of pathogens; (ii) a  
60 significant reduction in the volumes (70-80%); (iii) the accumulation and the  
61 concentration of the P content in the solid residues (Cieślik and Konieczka, 2017).  
62 Indeed, total P contents of char and ashes are usually comprised between 5 to 11%  
63 (dried mass), which is 1.2 to 2.6 times higher than the average P content of untreated SS  
64 (Herzel et al., 2016).

65 Several studies have investigated the potential of P recovery from char and ashes  
66 produced by incineration, gasification, and pyrolysis of SS (Atienza–Martínez et al.,  
67 2014; Donatello et al., 2010; Gorazda et al., 2018; Kleemann et al., 2017; Ottosen et al.,  
68 2013; Petzet et al., 2012; Xu et al., 2012). Most of these studies have focused on P  
69 extraction via acidic or alkaline leaching, and then P was recovered from the leachates

70 by chemical precipitation. However, many studies have focused only on equilibrium  
71 capacities, and further experiments are needed to model kinetics and mechanisms of P  
72 extraction. Moreover, only a few studies have dealt with P recovery from solid residues  
73 obtained by supercritical water gasification, supercritical water oxidation, and  
74 hydrothermal carbonation (Acelas et al., 2014; Huang and Tang, 2015; Stark et al.,  
75 2006), and there is a lack of data in the literature on P recovery from solid residues  
76 obtained by wet air oxidation of SS. Therefore, further experiments are needed to  
77 achieve a complete overview of P recovery potential of SS residues derived from the  
78 different current technologies.

79 This study aims at evaluating the potential of P recovery from solid residues obtained  
80 from wet air oxidation of SS under subcritical water conditions (WAO residues). A  
81 series of experiments of P extraction was performed by acidic and alkaline leaching at  
82 different liquid to solid ratios. Also, hot chemical extractions and P fractionations were  
83 carried out to characterize the chemical composition of the WAO residues. The main  
84 objectives of this study were (i) to determine the best operating conditions for P  
85 extraction, (ii) to determine the rate constants and maximum equilibrium capacities of P  
86 extraction, and (iii) to describe the main mechanisms leading to P extraction from the  
87 WAO residues. To the best of our knowledge, this paper represents the first complete  
88 study on capacity, kinetics, and mechanisms of P extraction from WAO residues.  
89 Knowledge and understanding of the kinetics and the main mechanisms of P extraction  
90 is indispensable to improve the design and the operation of the extraction process.

## 91 2 Material and methods

### 92 2.1 Samples collection and preparation

93 Solid residues used in this study derived from high temperature (235 °C) and pressure  
94 (4.5 MPa) wet air oxidation (WAO technology Athos, VEOLIA, France) of SS  
95 produced in the domestic WWTP of La Pioline (capacity 175000 population  
96 equivalent), located in Aix-en-Provence (France). The WAO residues were milled using  
97 a ceramic mortar to obtain particles with a size less than 0.5 mm and dried at 45 °C  
98 overnight to reduce their water content before the experiments. The temperature of 45  
99 °C was selected in order to reduce the risk of changes in the mineralogical composition  
100 during drying. The total water content of residues was determined after heating at 105  
101 °C until constant weight. This was done to determine the correct amount of WAO  
102 residue, based on dried mass equivalent, to be used in the different experiments.

### 103 2.2 Chemical characterization and P fractionation

104 A series of chemical extractions and elemental analyses were performed to investigate  
105 the chemical composition and quantify the different forms of P in the samples.

106 *Aqua regia* extractions were performed according to standard methods (EN 13346,  
107 2000; EN 13657, 2003) to investigate the elemental composition of the WAO residues.

108 *Aqua regia* dissolves metal oxides, hydroxides, carbonates, and metal phosphates.

109 Organic matter is digested and carbon is lost as CO<sub>2</sub>, while P and S are oxidized to  
110 phosphates and sulfates. A mixture of 1 g of WAO residue (dried mass equivalent) and  
111 28 mL of *aqua regia* was heated to 110 °C for two hours. Then, the mixture was filtered  
112 (0.45 µm filters) before elemental analyses. *Aqua regia* extractions were performed in  
113 duplicate. For each experiment, element extraction capacities q (mg/g) were determined

114 using equation (1), where C is the element concentration in the leachates (mg/L), V is  
115 the volume of extractant solution (L), and m is the dried mass of WAO residue (g).

$$116 \quad q = C \cdot L/m \quad (1)$$

117 A sequential extraction protocol, adapted by Tiessen and Moir (1993), was followed to  
118 quantify the fractions of P bound to different mineral compounds in the residues. Four  
119 fractions of P were sequentially extracted from 1 g of WAO residue (dried mass  
120 equivalent):

121 i. Bicarbonate extractable P was extracted in 20 mL of 0.5 M NaHCO<sub>3</sub>. This fraction is  
122 defined as weakly bound P, since the chemical changes introduced are minor and P  
123 extraction is mainly due to washing and ion exchange;

124 ii. Hydroxide extractable P was extracted in 20 mL of 0.1 M NaOH. This fraction is  
125 primarily related to dissolution of Al and Fe bound P compounds that are soluble at  
126 high, but insoluble at low pH;

127 iii. Diluted acid extractable P was extracted in 20 mL of 1 M HCl. This fraction is  
128 defined as Ca bound P, since Al and Fe bound P compounds that might remain after  
129 NaOH extraction are insoluble in acid;

130 iv. Hot concentrated acid extractable P was extracted in 12 mL of 10 M HCl in a 20 min  
131 water bath at 80 °C. This fraction represents P in stable residual compounds that need  
132 much more energy to be dissolved.

133 The fractions (i), (ii) and (iii) were determined after 16 h of rotary agitation at 5 r/min  
134 (rotary agitator STR4, Stuart, UK) at room temperature. After each extraction, the solid  
135 residues were washed with 20 mL of 1 M KCl to recover P re-adsorbed on the residue  
136 surface, and the KCl washes were added to the supernatant solution. Liquid samples

137 from each extraction were filtered (0.45  $\mu\text{m}$  filters) before elemental analyses. Then, for  
138 each step, P extraction capacities were determined by using equation (1). Sequential  
139 extractions were performed in duplicate.

140 Scanning electron microscopy observations coupled with energy dispersive X-ray  
141 spectroscopy analyses (SEM/EDX) were also performed to investigate the morphology  
142 and chemical composition of the residues. SEM/EDX analyses were carried out using a  
143 S-3000N scanning electron microscope model (Hitachi, Japan). All samples were dried  
144 at 45  $^{\circ}\text{C}$  overnight before SEM/EDX analyses.

## 145 2.3 *P extraction experiments*

### 146 2.3.1 *P extraction efficiency*

147 P extraction experiments (adapted from EN 12457-1 and 2, 2002) were performed using  
148 four different extractant solutions (1 M HCl, 1 M citric acid, 1 M acetic acid, and 0.1 M  
149 NaOH) at four different liquid to solid ratios (L/S) of 2, 5, 10, and 20 L/kg. The main  
150 objective was to establish the best extractant solution and L/S ratio for the P extraction.  
151 For each experiment, 100 mL of extractant solution were added into a series of four 200  
152 mL plastic bottles containing 5, 10, 20, and 50 g of WAO residues (dried mass  
153 equivalent). Then, the bottles were rotary agitated at 5 r/min at room temperature, and  
154 liquid samples were taken from each bottle after 24 h of agitation. All liquid samples  
155 were filtered (0.45  $\mu\text{m}$  filters) before elemental analyses. For each experiment, the 24 h  
156 element extraction capacities  $q$  (mg/g) were determined by using equation (1), as  
157 already described in the previous section. Element extraction efficiencies were then  
158 calculated as shown in equation (2), where  $q$  is the 24 h element extraction capacity by

159 acidic or alkaline leaching (mg/g), and  $q_{a.r.}$  is the element extraction capacity with *aqua*  
160 *regia* (mg/g).

$$161 \text{ Efficiency (\%)} = 100 \cdot q/q_{a.r.} \quad (2)$$

### 162 2.3.2 P extraction kinetics

163 A series of batch kinetic experiments was carried out to determine the maximum  
164 equilibrium capacities and the rate constants of P extraction from WAO residues.

165 Kinetic experiments were performed using 1 M citric acid and 1 M HCl at the L/S ratio  
166 of 10 L/kg. These operating conditions were selected based on the results of the  
167 comparative experiments (section 2.3.1). For each experiment, 700 mL of extractant  
168 solution were added into 1 L plastic bottles containing each 70 g of WAO residues  
169 (dried mass equivalent). Then, the bottles were rotary agitated at 5 r/min under room  
170 temperature, and liquid samples were collected from each bottle after 15, 30, 60, 120,  
171 180, and 240 min. Kinetic experiments were performed in duplicate. All the liquid  
172 samples were filtered (0.45  $\mu$ m filters) before elemental analyses, and for each sample  
173 element extraction capacities were determined by using equation (1). Experimental  
174 extraction capacities were then modelled using the integrated form of the pseudo second  
175 order kinetic equation as proposed by Ho and McKay (1998) (equation 3), where  $q_t$  is  
176 the extraction capacity at time  $t$  (mg/g),  $q_e$  is the extraction capacity at the equilibrium  
177 (mg/g), and  $k_2$  is the constant rate of the pseudo second order (g/(mg·min)).

$$178 \frac{t}{q_t} = \frac{1}{k_2 \cdot q_e^2} + \frac{1}{q_e} \cdot t \quad (3)$$

179 According to Ho and McKay (1998), the pseudo second order kinetic model efficiently  
180 describes a process primarily controlled by chemisorption (or chemidesorption) rather

181 than diffusion, with the concentration of one or more reagents that may become limiting  
182 the rate of the reaction over time.

#### 183 2.4 *Analytical methods*

184 Elemental analyses (Al, Ba, Ca, Cd, Co, Cr, Cu, Fe, K, Mg, Mn, Ni, P, Pb, Se, Si, V,  
185 and Zn) of liquid samples were performed by inductively coupled plasma atomic  
186 emission spectroscopy (ICP-AES) using a spectrometer Jobin Yvon Horiba Ultima-C  
187 (Horiba, Japan). For each set of analyses, limits of detection and limits of quantification  
188 were determined by analysis of blanks. All chemicals used were of analytical grade.

### 189 **3 Results and discussion**

#### 190 3.1 *Chemical characterization and P fractionation*

191 The results of *aqua regia* extractions indicated that Ca, Fe, P, Mg, and Al represent at  
192 least 49.5% of the total mass of dried WAO residues (Table 1). Ca, Fe, P, Mg, and Al  
193 extraction capacities with *aqua regia* were  $170 \pm 2$  mg Ca/g WAO residue,  $150 \pm 1$  mg  
194 Fe/g WAO residue,  $132 \pm 1$  mg P/g WAO residue,  $22.9 \pm 0.1$  mg Mg/g WAO residue,  
195 and  $19.8 \pm 0.2$  mg Al/g WAO residue, respectively (average values  $\pm$  standard deviation  
196 from duplicate experiments). Ca and Mg in WAO residues were most probably  
197 primarily related to the Ca and Mg contents of wastewater and biomass, whereas Fe and  
198 Al likely derived from the use of Fe and Al salts to improve P removal from wastewater  
199 by chemical precipitation in the WWTP. Moreover, *aqua regia* extractions indicated a  
200 significant presence of K ( $3.0 \pm 0.2$  mg/g), Cu ( $2.5 \pm 0.1$  mg/g), and Zn ( $2.08 \pm 0.02$   
201 mg/g), which are essential micronutrients for biomass growth and they are classically  
202 present in little amounts among the components of SS. Furthermore, the results in Table  
203 1 suggest that other elements such as Ba, Cd, Co, Cr, Mn, Ni, Pb, Se, and V were

204 present only in trace in WAO residues, and their concentrations in the *aqua regia*  
205 leachates were often very close to the limits of quantification for the analyses.

206 Sequential extraction experiments indicated that the main fraction of P in WAO  
207 residues was Ca bound P, representing the 86.3% of the total mass of P extracted,  
208 followed by P in stable compounds (8.9%), and Al and Fe bound P (3.5%) (Figure 1). In  
209 the literature (Barca et al., 2014; Drizo et al., 2002; Tiessen and Moir, 1993), Ca bound  
210 P is mainly attributed to amorphous Ca phosphates and/or less stable Ca phosphates,  
211 such as dicalcium phosphate (DCP), octacalcium phosphate (OCP), and tricalcium  
212 phosphate (TCP), which can be dissolved with diluted acids (*e.g.* 1 M HCl), whereas the  
213 residual P in stable compounds can be referred to more thermodynamically stable Ca-P  
214 crystals (*e.g.* hydroxyapatite) and/or P from stable organic matter that is not alkaline  
215 extractable (Drizo et al., 2002; Thomsen et al., 2017; Tiessen and Moir, 1993).

216 A large number of studies have investigated the P composition of SS residues derived  
217 from various types of thermal treatments (Table 2). The data indicate that the total P  
218 content of SS residues may vary into a large range of values, from 27 to 119 g P/kg  
219 (Stark et al., 2006; Xu et al., 2012), depending on the type of the thermal process, on the  
220 temperature and pressure conditions of the process, and on the initial P composition of  
221 SS (Kleemann et al., 2017; Tan and Lagerkvist, 2011; Thomsen et al., 2017). During SS  
222 incineration at temperatures ranging between 800-900 °C, organic P volatilizes to form  
223 volatile oxides that re-condense upon temperature decreases at 400-600 °C, and it is  
224 recovered as inorganic Ca, Al, and/or Fe phosphates in the fly ashes (Cieślik and  
225 Konieczka, 2017; Magdziarz et al., 2016; Niu and Shen, 2018), while inorganic Fe-P  
226 and Al-P pools are oxidized to new P complexes (mainly Ca phosphates) and residual  
227 pools of Fe and Al oxides (Atienza–Martínez et al., 2014; Li et al., 2017; Parés Viader

228 et al., 2017b; Thomsen et al., 2017). The addition of CaO during SS incineration may  
229 promote the transformation of inorganic Fe-P and Al-P pools to Ca-P complexes and  
230 residual Fe and Al oxides, as demonstrated by Li et al. (2017). As a result of these  
231 mineralogical changes, inorganic Ca-P pools often represent the main P fraction in solid  
232 residues from SS incineration (Donatello et al., 2010; Li et al., 2017, 2015; Magdziarz  
233 et al., 2016). Similar trends were also observed for SS residues from gasification and  
234 pyrolysis processes (Acelas et al., 2014; Kleemann et al., 2017; Parés Viader et al.,  
235 2017b; Thomsen et al., 2017).

236 The results of this study indicate that the P content of WAO residues is higher than the  
237 average P content of SS residues tested in previous studies (Table2), and P in WAO  
238 residues is mainly present as Ca bound P. Most probably, the relatively lower  
239 temperature (235 °C) and higher pressure (4.5 MPa) conditions of the WAO process  
240 had the effect of (i) avoiding the volatilization of organic P and (ii) promoting its  
241 conversion to inorganic Ca-P complexes, thus leading to a significant increment in the P  
242 content of the residues. The results of SEM/EDX indicated that WAO residues are  
243 primarily composed of O, Ca, P, and Fe (Figure 1S, supplementary material), and  
244 elemental maps confirmed the presence of Ca-P pools covering the full surface of the  
245 samples (Figure 2S, supplementary material). Furthermore, SEM observations revealed  
246 that WAO residues are composed of amorphous aggregates with rare crystalline phases,  
247 suggesting that Ca-P complexes are mainly present as amorphous phases. There is a  
248 large discrepancy in the literature concerning the main crystalline and amorphous  
249 phases that are present in the residues from thermal treatments of SS. Overall, many  
250 studies have indicated that quartz ( $\text{SiO}_2$ ), calcite ( $\text{CaCO}_3$ ), and hematite ( $\text{Fe}_2\text{O}_3$ ) are the  
251 prevalent crystalline phases, whereas Ca-P pools are often present as amorphous or

252 poorly crystallized aggregates (Atienza–Martínez et al., 2014; Donatello et al., 2010;  
253 Magdziarz et al., 2016).

### 254 3.2 P extraction efficiency

255 Figure 2 shows the P extraction efficiencies observed after 24 h of contact time as a  
256 function of the liquid to solid ratio (L/S) for the different extractant solutions that were  
257 tested. The results clearly indicated that the best extractants for P extraction were 1 M  
258 citric acid and 1 M HCl at the L/S ratio of 10 L/kg. Indeed, 1 M citric acid and 1 M HCl  
259 at the L/S ratio of 10 L/kg extracted 86.4 mg P/g WAO and 92.0 mg P/g WAO,  
260 respectively, representing 65% and 70% of the total mass of P extracted with *aqua regia*  
261 (Table 1). A further increase in L/S ratio to 20 L/kg did not lead to a significant increase  
262 in P extraction efficiencies (Figure 2).

263 The lowest P extraction efficiencies (< 2.5%) were observed when using 0.1 M NaOH  
264 as solvent. This is in good agreement with the findings of previous studies (Biswas et  
265 al., 2009; Stark et al., 2006; Xu et al., 2012), which have indicated that NaOH is not an  
266 effective solvent for P extraction from SS residues.

267 The pH values of the leachates after 24 h of extraction ranged between 1.1-2.8 for 1 M  
268 HCl, 2.2-2.8 for 1 M citric acid, 3.3-4.0 for 1 M acetic acid, and 10.2-12.4 for 0.1 M  
269 NaOH (Table S1, supplementary material). These results seem to confirm that Ca bound  
270 P represents the main fraction of P in WAO residues, and that P extraction was  
271 primarily due to dissolution of Ca-P complexes under acidic conditions. Indeed,  
272 solubility of Ca phosphates drastically increases with decreasing pH below 4 (Stumm  
273 and Morgan, 2012), and they are much more soluble under acidic rather than alkaline  
274 conditions. According to the supposed mechanism of P extraction, the higher pH values

275 of the leachates for 1 M acetic acid may account for its lower P extraction efficiency  
276 compared to those of 1 M citric acid and 1 M HCl (Figure 2).

277 Figure 3 shows the evolution of P concentrations and pH values of the leachates after 24  
278 h of contact time as a function of the L/S ratio when using 1 M citric acid and 1 M HCl  
279 as extractant solutions. The results seem to confirm that the L/S ratio of 10 L/kg was the  
280 optimum operating condition for combining high P extraction efficiencies (> 60%) with  
281 high P concentrations in the leachates (> 8 g P/L). Moreover, the results shown in  
282 Figure 3 indicate that 1 M citric acid may give higher P concentrations than those  
283 obtained with 1 M HCl at similar pH values of the leachates, especially when using a  
284 L/S ratio lower than 10 L/kg. This was most probably due to the metal chelating  
285 properties of citric acid, which may have the effect of preventing the precipitation of  
286 metal phosphates after P extraction, thus improving the effective solubility of P in the  
287 leachates.

288 Table 1 summarizes the element extraction capacities and efficiencies using 1 M citric  
289 acid and 1 M HCl at the L/S ratio of 10 L/kg after 24 h of contact time compared to  
290 *aqua regia* extractions. The highest extraction efficiencies were observed for Ca (>  
291 78%) and P (> 65%), whereas the extraction efficiencies of the other elements that are  
292 present in greater amounts in the composition of WAO residues (Al, Fe, and Mg) were  
293 always lower than 24% for Al, 28% for Fe, and 55% for Mg. These results seem to  
294 indicate a higher affinity of 1 M citric acid and 1 M HCl for the dissolution of Ca-P  
295 complexes rather than Al and/or Fe complexes, as already found in previous studies  
296 (Biswas et al., 2009; Petzet et al., 2012), most probably because: (i) Fe oxides produced  
297 during thermal treatments of SS (*e.g.* hematite) are usually acid-insoluble (Thomsen et

298 al., 2017), and (ii) Ca phosphates are several orders of magnitude more soluble than Al  
299 and Fe phosphates at pH lower than 4 (Stumm and Morgan, 2012).

300 As shown in Table 1, 1 M HCl has shown a P extraction capacity 1.06 times higher than  
301 1 M citric acid, while 1 M citric acid has shown Zn and Cu extraction capacities 1.47-  
302 1.70 times higher than 1 M HCl. This was most probably due to the metal chelating  
303 properties of citric acid that may have favored extraction of Zn and Cu from WAO  
304 residue, as already observed in comparative studies that tested the use of weak organic  
305 acids to extract heavy metals from polluted soils (Wasay et al., 2001).

306 It should be also noticed that 1 M citric acid and 1 M HCl have shown very higher Si  
307 extraction capacities than *aqua regia*. Indeed, silicate minerals are usually recalcitrant to  
308 dissolution by *aqua regia* and they remain in solid form (Chen and Ma, 2001).

309 However, P extraction capacities with 1 M citric acid and 1 M HCl were lower than  
310 those observed with *aqua regia* (Table 1), and they were in good agreement with the  
311 findings of P fractionation (Figure 1). This suggests that the amount of P extracted by  
312 dissolution of silicate minerals was negligible compared to the amount of P extracted by  
313 dissolution of Ca-P compounds.

314 Table 2 summarizes the optimum operating parameters and the main experimental  
315 results of recent studies that have investigated the P extraction from various types of SS  
316 residues. As shown in Table 2, it is difficult to compare the results of the different  
317 studies because of the large variety on the origin and chemical compositions of the  
318 residues, and the discrepancy between the experimental parameters that were  
319 established for the extractions. Many studies have focused on ashes from incineration,  
320 and only a few have dealt with SS residues from gasification, pyrolysis, and  
321 supercritical water processes. Most of the studies have indicated optimum extraction

322 conditions with inorganic acids (HCl, H<sub>2</sub>SO<sub>4</sub>, HNO<sub>3</sub>) at concentrations ranging from  
323 0.05 to 2.7 M and L/S ratios from 2 to 150 L/kg. Only two studies have tested organic  
324 acids (oxalic acid)(Acelas et al., 2014; Atienza–Martínez et al., 2014), and only one  
325 study has found high extraction efficiency (> 70%) with an alkaline solvent (1 M  
326 NaOH), but this after an acidic pretreatment of the residues to promote the mobilization  
327 of Ca bound P (Petzet et al., 2012). The main mechanism of P extraction was attributed  
328 to the dissolution of various P compounds (mainly Ca phosphates) that are soluble  
329 under acidic conditions (Donatello et al., 2010; Kleemann et al., 2017; Li et al., 2015).  
330 Therefore, a high fraction of Ca bound P is considered as a positive predictive factor  
331 when evaluating the potential of P recovery from a residue. Overall, there is a good  
332 agreement in the literature concerning the optimum contact time for P extraction from  
333 SS residues, and usually the extraction efficiencies stabilize around a value ranging  
334 between 80% and 90% after 2 h of contact time (Table 2).

335 As shown in Table 1 and 2, P extraction efficiencies of this study were lower, while P  
336 extraction capacities were higher than those observed in previous studies. This seems to  
337 indicate that WAO residues contain a higher fraction of P that is recalcitrant to acidic  
338 leaching compared to the other types of SS residues. This fraction may be primarily  
339 attributed to more thermodynamically stable Ca-P crystals (*e.g.* hydroxyapatite) and to  
340 P in stable residual organic compounds, as already suggested by the results of P  
341 fractionation (Figure 1). Indeed, P bound to residual organic compounds is usually inert  
342 to acidic and basic leaching (Acelas et al., 2014). The higher fraction of P recalcitrant to  
343 acidic extraction in WAO residues was probably related to the relatively lower  
344 temperature of the WAO process, which may have led to an incomplete conversion of  
345 organic P. Indeed, comparative experiments of supercritical water gasification (SCWG)

346 of SS have confirmed that the higher the SCWG temperature, the more organic P is  
347 converted into inorganic leachable P (Acelas et al., 2014).

### 348 3.3 *P extraction kinetics*

349 Kinetic experiments of P extraction were carried out using 1 M HCl and 1 M citric acid  
350 at the L/S ratio of 10 L/kg, which represent the optimum extraction conditions that were  
351 established by the previous experiments (section 3.2). Figure 4 shows the evolution of  
352 experimental extraction capacities of Ca and P as a function of the time for the  
353 experiments performed with 1 M HCl (Figure 4A) and 1 M citric acid (Figure 4B). The  
354 results indicate that a pseudo-equilibrium in P extraction was achieved after 1 h for 1 M  
355 HCl and after 2 h for 1 M citric acid, with P extraction capacities stabilizing around a  
356 value of 80 mg P/g WAO residue. These results are in good agreement with the finding  
357 of previous studies (Table 2), which have shown optimum contact times of around 2 h.

358 Table 3 summarizes the main results of modelling experimental extraction capacities of  
359 Ca and P by the use of the pseudo-second order kinetic equation of Ho and McKay  
360 (1998). The very high coefficients of correlation ( $R^2 > 0.998$ ) indicate that the model  
361 describes the experimental data very well. Moreover, the equilibrium extraction  
362 capacities of Ca and P obtained by the model (Table 3) were in good agreement with the  
363 experimental capacities observed after 24 h of contact time (Table 1), thus confirming  
364 the validity of the model. Furthermore, the kinetic constants  $k_2$  of Ca and P extractions  
365 with 1 M HCl were 4-5 times higher than those obtained with 1 M citric acid (Table 3),  
366 confirming that P extraction using 1 M HCl is faster than using 1 M citric acid.  
367 However, despite P extraction with 1 M HCl being faster, the results shown in Figure 4  
368 and Table 3 suggest that maximum P extraction capacities at the equilibrium may be  
369 higher when using 1 M citric acid as solvent. This was probably due to the metal

370 chelating properties of citric acid which may have improved (i) the capacities of metal  
371 bound P extraction at the equilibrium, and (ii) the effective solubility of P in the  
372 leachates, as already discussed in the previous sections.

373 Overall, the experimental and modelled results seem to indicate a clear correlation  
374 between Ca and P extraction from WAO residues, whereas no correlations were found  
375 between P extraction and the extraction of Fe and Al. This appears to further confirm  
376 that P extraction was mainly due to dissolution of Ca-P complexes under acidic  
377 conditions.

#### 378 3.4 *P extraction mechanisms*

379 According to Ho and McKay (1998), if the pseudo-second order model well describes  
380 the kinetic data, this may indicate that P release from the WAO residues was primarily  
381 controlled by the chemical reaction rather than diffusion, with one or more reagents that  
382 can become limiting the rate of the extraction over time. However, recent studies have  
383 shown that a good mathematical description of experimental data is not sufficient  
384 enough to validate the underlying mechanisms of the model, and more caution should  
385 be paid to the analysis of kinetic data (Simonin, 2016).

386 For these reasons, experimental data were further analyzed in order to fully understand  
387 the main mechanisms leading to P extraction from WAO residues. As shown in Figure  
388 5, a very good direct correlation between moles of Ca extracted and moles of P  
389 extracted was observed during kinetic experiments. The molar ratios of Ca to P  
390 extracted were 1.34 Ca/P and 1.31 Ca/P when using 1 M HCl and 1 M citric acid,  
391 respectively. These molar ratios were in the range of molar ratios Ca/P of the most  
392 common Ca phosphates in wastewater treatment systems (Table 4), and this appears to

393 confirm that P extraction was primarily due to the dissolution of a mixture of various  
394 Ca-P complexes.

395 Table 4 summarizes formula, molar ratios Ca/P, and solubility constants of various Ca  
396 phosphates. Among the crystalline forms, the most soluble are dicalcium phosphates  
397 (DCP) and tricalcium phosphates (TCP). Solubility of amorphous calcium phosphates  
398 (ACP) is variable, but usually they are more soluble than crystalline phases (Valsami-  
399 Jones, 2001). The findings of this study seem to indicate that dissolution of ACP was  
400 the most probable mechanism leading to P extraction, as SEM observations revealed  
401 that WAO residues were predominantly composed of amorphous aggregates. Moreover,  
402 experimental molar ratios of Ca/P extracted (1.31-1.34) were very consistent with the  
403 theoretical molar ratio of Ca/P for the dissolution of a mixture of various ACP (Table  
404 4).

405 Overall, the results of this study seem to confirm that P extraction from WAO residues  
406 was a process primarily controlled by the dissolution of Ca phosphates, with Ca  
407 phosphates that can become limiting the rate of the extraction over time. This  
408 hypothesis is further supported by the very good agreement between the amount of Ca  
409 bound P on WAO residues (Figure 1) and the equilibrium capacities of Ca and P  
410 extraction (Table 3), which indicate that Ca phosphates were no longer available for  
411 dissolution after 4 h of contact time.

#### 412 **4 Closing remarks and perspectives**

413 The results of this study have indicated a high potential for P recovery from WAO  
414 residues using 1 M citric acid and 1 M HCl as extractant solutions. Despite HCl shows a  
415 faster P extraction kinetic, the use of citric acid presents several advantages compared to

416 HCl, as (i) citric acid is a bio-sourced product that can be produced in large amounts in  
417 bioreactors by cultivation of microorganisms (*e.g. Aspergillus niger*), and (ii) it is  
418 highly biodegradable, thus facilitating the treatment and management of the effluents  
419 from the process.

420 However, as shown in Table 1, significant amounts of heavy metals (in particular Fe,  
421 Al, Cu, and Zn) were extracted from WAO residues, whose presence in the leachates is  
422 unbeneficial as it may affect the purity and quality of the P recovered. A large variety of  
423 separation techniques have been proposed in the literature to recover and concentrate P  
424 from the leachates of acidic extractions. Among the different techniques, sequential  
425 precipitation with increasing step by step the pH of the leachates was one of the most  
426 employed to recover P in the form of pure Ca-phosphates (Kaikake et al., 2009;  
427 Kalmykova and Fedje, 2013; Petzet et al., 2012). Other authors have proposed the use  
428 of cation exchange resins to remove heavy metals from the leachates and hence obtain  
429 metal free solutions (Donatello et al., 2010; Franz, 2008; Xu et al., 2012). Biswas et al.  
430 (2009) obtained good efficiencies of P recovery from the leachates by selective  
431 adsorption on orange waste gel.

432 Thermochemical pre-treatments of SS residues may also represent a suitable alternative  
433 solution to remove metals from the residues and improve P bioavailability and/or  
434 leachability (Adam et al., 2009; Havukainen et al., 2016; Krüger and Adam, 2015).  
435 Adam et al. (2009) indicated that a thermal pretreatment of ashes at temperatures of  
436 about 1000 °C can effectively remove heavy metals by volatilization due to their high  
437 vapor pressures, while P bound to stable mineral phases is transformed to more soluble  
438 Ca and Mg phosphates.

439 In recent years, the development of membrane-based electro dialytic processes for  
440 simultaneous separation of P and heavy metals from the leachates has received  
441 increasing attention from the scientific community (Ebbbers et al., 2015; Guedes et al.,  
442 2016; Parés Viader et al., 2017a; Villen-Guzman et al., 2018). Parés Viader et al.  
443 (2017a) indicated that the recovery of Al- and Fe-free P from Al- and Fe-rich ashes can  
444 be increased by a factor of two with a sequential electro dialytic process that alternates a  
445 first step of acidic extraction followed by a second step of alkaline extraction.

446 According to the data published in the literature, sequential precipitation appears to be  
447 the most robust technique to recover pure Ca-P precipitates from the leachates due to  
448 the simplicity and relatively low operating costs of the process. Nevertheless, it should  
449 be noted that metal chelating properties of certain organic acids and residual organic  
450 compounds may inhibit and/or alter the stability of Ca-P precipitation (Valsami-Jones,  
451 2001), thus affecting kinetics and efficiency of the process. Therefore, the use of  
452 membrane-based and electrically-driven processes such as electro dialysis seems to be  
453 more appropriate to achieve efficient separation of phosphates and heavy metals from  
454 the leachates, especially when using 1 M citric acid as extractant solution.

455 However, despite numerous studies have demonstrated the effectiveness of these  
456 separation techniques at the laboratory scale, today the number of pilot and industrial  
457 scale applications is still scarce (Krüger and Adam, 2015). A comparative study on life  
458 cycle assessment (LCA) and life cycle cost analysis (LCC) for the different processes,  
459 based on the results of full scale applications, would be required to thoroughly identify  
460 the advantages and limitations of each technique.

## 461 **5 Conclusions**

462 The results of this study confirm that SS residues of WAO are a promising secondary P  
463 source for fertilizer production. *Aqua regia* extractions and P fractionation experiments  
464 revealed a total P content of WAO residues of about  $132 \pm 1$  g P/kg, with P mainly  
465 present as Ca bound P. Optimum conditions for P extraction were observed when using  
466 1 M citric acid and 1 M HCl at L/S ratio of 10 L/kg as extractant solutions at room  
467 temperature. After 2 h of contact time, P extraction efficiencies were 61% and 65%,  
468 giving P extraction capacities of 81 and 86 g P/kg of WAO for 1 M citric acid and 1 M  
469 HCl, respectively. The kinetic analysis of experimental data by the use of the pseudo-  
470 second order kinetic model indicates that P extraction with 1 M HCl is faster, but 1 M  
471 citric acid may give higher capacities of P extraction at the equilibrium. Molar ratios of  
472 Ca to P extracted from WAO residues ranged around 1.31-1.34 mol Ca/mol P,  
473 suggesting that P extraction was primarily due to dissolution of a mixture of various Ca-  
474 P complexes (most probably amorphous Ca phosphates) under acidic conditions. Al and  
475 Fe extraction efficiencies have been always lower than 28%, and no correlations were  
476 observed between the extraction of these metals and the extraction of P, thus indicating  
477 that 1 M citric acid and 1 M HCl have a higher affinity for the dissolution of Ca  
478 phosphates rather than Al and Fe complexes.

## 479 **Acknowledgements**

480 This project has received the support and has been founded by ECCOREV Research  
481 Federation (FR 3098 Aix Marseille Univ-CNRS). We thank H el ene Miche and Bertrand  
482 Devouard (CEREGE, France) for elemental analyses and SEM/EDX observations.

## 483 **Supplementary material**

484 Figure S1. SEM/EDX analysis: elemental spectrum for WAO residues.  
485 Figure S2. SEM/EDX analysis: elemental maps of Ca (A) and P (B) for the same sample  
486 of WAO residue.  
487 Table S1. pH values and P concentrations of the leachates after 24 h of extraction as a  
488 function of the liquid to solid ratio (L/S) for different extractant solutions.

#### 489 **References**

490 Acelas, N.Y., López, D.P., Brilman, D.W.F. (Wim), Kersten, S.R.A., Kootstra, A.M.J.,  
491 2014. Supercritical water gasification of sewage sludge: Gas production and phosphorus  
492 recovery. *Bioresource Technology* 174, 167–175.  
493 <https://doi.org/10.1016/j.biortech.2014.10.003>

494 Adam, C., Peplinski, B., Michaelis, M., Kley, G., Simon, F.-G., 2009. Thermochemical  
495 treatment of sewage sludge ashes for phosphorus recovery. *Waste management* 29, 1122–  
496 1128.

497 Atienza–Martínez, M., Gea, G., Arauzo, J., Kersten, S.R.A., Kootstra, A.M.J., 2014.  
498 Phosphorus recovery from sewage sludge char ash. *Biomass and Bioenergy*, 21st  
499 European Biomass Conference 65, 42–50.  
500 <https://doi.org/10.1016/j.biombioe.2014.03.058>

501 Barca, C., Meyer, D., Liira, M., Drissen, P., Comeau, Y., Andrès, Y., Chazarenc, F., 2014.  
502 Steel slag filters to upgrade phosphorus removal in small wastewater treatment plants:  
503 Removal mechanisms and performance. *Ecological Engineering* 68, 214–222.  
504 <https://doi.org/10.1016/j.ecoleng.2014.03.065>

505 Biswas, B.K., Inoue, K., Harada, H., Ohto, K., Kawakita, H., 2009. Leaching of  
506 phosphorus from incinerated sewage sludge ash by means of acid extraction followed by  
507 adsorption on orange waste gel. *Journal of Environmental Sciences* 21, 1753–1760.

508 Chen, M., Ma, L.Q., 2001. Comparison of Three Aqua Regia Digestion Methods for  
509 Twenty Florida Soils. *Soil Science Society of America Journal* 65, 491–499.  
510 <https://doi.org/10.2136/sssaj2001.652491x>

511 Cieřlik, B., Konieczka, P., 2017. A review of phosphorus recovery methods at various  
512 steps of wastewater treatment and sewage sludge management. The concept of “no solid  
513 waste generation” and analytical methods. *Journal of Cleaner Production* 142, 1728–  
514 1740. <https://doi.org/10.1016/j.jclepro.2016.11.116>

515 Cordell, D., Rosemarin, A., Schröder, J., Smit, A., 2011. Towards global phosphorus  
516 security: A systems framework for phosphorus recovery and reuse options. *Chemosphere*  
517 84, 747–758.

518 Desmidt, E., Ghyselbrecht, K., Zhang, Y., Pinoy, L., Bruggen, B.V. der, Verstraete, W.,  
519 Rabaey, K., Meesschaert, B., 2015. Global Phosphorus Scarcity and Full-Scale P-  
520 Recovery Techniques: A Review. *Critical Reviews in Environmental Science and*  
521 *Technology* 45, 336–384. <https://doi.org/10.1080/10643389.2013.866531>

522 Donatello, S., Tong, D., Cheeseman, C.R., 2010. Production of technical grade  
523 phosphoric acid from incinerator sewage sludge ash (ISSA). *Waste management* 30,  
524 1634–1642.

525 Drizo, A., Comeau, Y., Forget, C., Chapuis, R.P., 2002. Phosphorus saturation potential:  
526 a parameter for estimating the longevity of constructed wetland systems. *Environ. Sci.*  
527 *Technol.* 36, 4642–4648.

528 Ebbers, B., Ottosen, L.M., Jensen, P.E., 2015. Comparison of two different electro-dialytic  
529 cells for separation of phosphorus and heavy metals from sewage sludge ash.  
530 *Chemosphere* 125, 122-129. <https://doi.org/10.1016/j.chemosphere.2014.12.013>

531 Franz, M., 2008. Phosphate fertilizer from sewage sludge ash (SSA). *Waste Management*  
532 28, 1809–1818. <https://doi.org/10.1016/j.wasman.2007.08.011>

533 Gorazda, K., Tarko, B., Werle, S., Wzorek, Z., 2018. Sewage sludge as a fuel and raw  
534 material for phosphorus recovery: Combined process of gasification and P extraction.  
535 *Waste Management* 73, 404–415. <https://doi.org/10.1016/j.wasman.2017.10.032>

536 Guedes, P., Couto, N., Ottosen, L.M., Kirkelund, G.M., Mateus, E., Ribeiro, A.B., 2016.  
537 Valorisation of ferric sewage sludge ashes: Potential as a phosphorus source. *Waste*  
538 *Management* 52, 193–201. <https://doi.org/10.1016/j.wasman.2016.03.040>

539 Havukainen, J., Nguyen, M.T., Hermann, L., Horttanainen, M., Mikkilä, M., Deviatkin,  
540 I., Linnanen, L., 2016. Potential of phosphorus recovery from sewage sludge and manure  
541 ash by thermochemical treatment. *Waste Management* 49, 221–229.  
542 <https://doi.org/10.1016/j.wasman.2016.01.020>

543 Herzel, H., Krüger, O., Hermann, L., Adam, C., 2016. Sewage sludge ash — A promising  
544 secondary phosphorus source for fertilizer production. *Science of The Total Environment*  
545 542, 1136–1143. <https://doi.org/10.1016/j.scitotenv.2015.08.059>

546 Ho, Y.S., McKay, G., 1998. A Comparison of Chemisorption Kinetic Models Applied to  
547 Pollutant Removal on Various Sorbents. *Process Safety and Environmental Protection*  
548 76, 332–340. <https://doi.org/10.1205/095758298529696>

549 Huang, R., Tang, Y., 2015. Speciation dynamics of phosphorus during (Hydro)Thermal  
550 treatments of sewage sludge. *Environmental Science and technology* 49, 14466-14474.  
551 DOI: 10.1021/acs.est.5b04140.

552 Kaikake, K., Sekito, T., Dote, Y., 2009. Phosphate recovery from phosphorus-rich  
553 solution obtained from chicken manure incineration ash. *Waste Management* 29, 1084–  
554 1088.

555 Kalmykova, Y., Fedje, K.K., 2013. Phosphorus recovery from municipal solid waste  
556 incineration fly ash. *Waste management* 33, 1403–1410.

557 Kleemann, R., Chenoweth, J., Clift, R., Morse, S., Pearce, P., Saroj, D., 2017.  
558 Comparison of phosphorus recovery from incinerated sewage sludge ash (ISSA) and  
559 pyrolysed sewage sludge char (PSSC). *Waste Management* 60, 201–210.  
560 <https://doi.org/10.1016/j.wasman.2016.10.055>

561 Krüger, O., Adam, C., 2015. Recovery potential of German sewage sludge ash. *Waste*  
562 *Management* 45, 400–406. <https://doi.org/10.1016/j.wasman.2015.01.025>

563 Li, R., Teng, W., Li, Y., Wang, W., Cui, R., Yang, T., 2017. Potential recovery of  
564 phosphorus during the fluidized bed incineration of sewage sludge. *Journal of Cleaner*  
565 *Production* 140, 964–970. <https://doi.org/10.1016/j.jclepro.2016.06.177>

566 Li, R., Zhang, Z., Li, Y., Teng, W., Wang, W., Yang, T., 2015. Transformation of apatite  
567 phosphorus and non-apatite inorganic phosphorus during incineration of sewage sludge.  
568 *Chemosphere* 141, 57–61. <https://doi.org/10.1016/j.chemosphere.2015.05.094>

569 Magdziarz, A., Wilk, M., Gajek, M., Nowak-Woźny, D., Kopia, A., Kalemba-Rec, I.,  
570 Koziński, J.A., 2016. Properties of ash generated during sewage sludge combustion: A  
571 multifaceted analysis. *Energy* 113, 85–94. <https://doi.org/10.1016/j.energy.2016.07.029>

572 Melia, P.M., Cundy, A.B., Sohi, S.P., Hooda, P.S., Busquets, R., 2017. Trends in the  
573 recovery of phosphorus in bioavailable forms from wastewater. *Chemosphere* 186, 381–  
574 395. <https://doi.org/10.1016/j.chemosphere.2017.07.089>

575 Niu, X., Shen, L., 2018. Release and transformation of phosphorus in chemical looping  
576 combustion of sewage sludge. *Chemical Engineering Journal* 335, 621–630.  
577 <https://doi.org/10.1016/j.cej.2017.11.015>

578 Ottosen, L.M., Kirkelund, G.M., Jensen, P.E., 2013. Extracting phosphorous from  
579 incinerated sewage sludge ash rich in iron or aluminum. *Chemosphere* 91, 963–969.  
580 <https://doi.org/10.1016/j.chemosphere.2013.01.101>

581 Parés Viader, R., Jensen, P.E., Ottosen, L.M., Ahrenfeldt, J., Hauggaard-Nielsen, H.,  
582 2017a. Sequential electro-dialytic recovery of phosphorus from low-temperature  
583 gasification ashes of chemically precipitated sewage sludge. *Waste Management* 60, 211–  
584 218. <https://doi.org/10.1016/j.wasman.2016.11.030>

585 Parés Viader, R., Jensen, P.E., Ottosen, L.M., Thomsen, T.P., Ahrenfeldt, J., Hauggaard-  
586 Nielsen, H., 2017b. Comparison of phosphorus recovery from incineration and  
587 gasification sewage sludge ash. *Water Sci Technol* 75, 1251–1260.  
588 <https://doi.org/10.2166/wst.2016.620>

589 Petzet, S., Peplinski, B., Cornel, P., 2012. On wet chemical phosphorus recovery from  
590 sewage sludge ash by acidic or alkaline leaching and an optimized combination of both.  
591 *Water research* 46, 3769–3780.

592 Simonin, J.-P., 2016. On the comparison of pseudo-first order and pseudo-second order  
593 rate laws in the modeling of adsorption kinetics. *Chemical Engineering Journal* 300, 254–  
594 263. <https://doi.org/10.1016/j.cej.2016.04.079>

595 Sørensen, B.L., Dall, O.L., Habib, K., 2015. Environmental and resource implications of  
596 phosphorus recovery from waste activated sludge. *Waste Management, Urban Mining* 45,  
597 391–399. <https://doi.org/10.1016/j.wasman.2015.02.012>

598 Stark, K., Plaza, E., Hultman, B., 2006. Phosphorus release from ash, dried sludge and  
599 sludge residue from supercritical water oxidation by acid or base. *Chemosphere* 62, 827–  
600 832. <https://doi.org/10.1016/j.chemosphere.2005.04.069>

601 Stumm, W., Morgan, J.J., 2012. *Aquatic Chemistry: Chemical Equilibria and Rates in*  
602 *Natural Waters*. John Wiley & Sons.

603 Tan, Z., Lagerkvist, A., 2011. Phosphorus recovery from the biomass ash: A review.  
604 *Renewable and Sustainable Energy Reviews* 15, 3588–3602.

605 Thomsen, T.P., Sárossy, Z., Ahrenfeldt, J., Henriksen, U.B., Frandsen, F.J., Müller-  
606 Stöver, D.S., 2017. Changes imposed by pyrolysis, thermal gasification and incineration  
607 on composition and phosphorus fertilizer quality of municipal sewage sludge. *Journal of*  
608 *Environmental Management* 198, 308–318.  
609 <https://doi.org/10.1016/j.jenvman.2017.04.072>

610 Tiessen, H., Moir, J.O., 1993. Characterization of available P by sequential extraction.  
611 *Soil sampling and methods of analysis* 7, 5–229.

612 Valsami-Jones, E., 2001. Mineralogical controls on phosphorus recovery from  
613 wastewaters. *Mineralogical Magazine* 65, 611–620.  
614 <https://doi.org/10.1180/002646101317018433>

615 Villen-Guzman, M., Guedes, P., Couto, N., Ottosen, L.M., Ribeiro, A.B., Rodriguez-  
616 Maroto, J.M., 2018. Electrodialytic phosphorus recovery from sewage sludge ash under  
617 kinetic control. *Electrochimica Acta*. <https://doi.org/10.1016/j.electacta.2018.08.032>

618 Wasay, S.A., Barrington, S., Tokunaga, S., 2001. Organic Acids for the In Situ  
619 Remediation of Soils Polluted by Heavy Metals: Soil Flushing in Columns. *Water, Air,  
620 & Soil Pollution* 127, 301–314. <https://doi.org/10.1023/A:1005251915165>

621 Xu, H., He, P., Gu, W., Wang, G., Shao, L., 2012. Recovery of phosphorus as struvite  
622 from sewage sludge ash. *Journal of Environmental Sciences* 24, 1533–1538.  
623 [https://doi.org/10.1016/S1001-0742\(11\)60969-8](https://doi.org/10.1016/S1001-0742(11)60969-8)

624

625

626 **Table captions**

627 Table 1. Element extraction capacities and efficiencies using 1 M citric acid and 1 M  
628 HCl after 24 h of contact time compared to aqua regia extraction capacities.

629 Table 2. Main results of recent studies that have investigated P extraction from solid  
630 residues derived from thermal treatments of SS: ISS = incineration SS; PSS = pyrolysis  
631 SS; GSS = gasification SS; HTC = hydrothermal carbonization; SCWO = supercritical  
632 water oxidation; SCWG = supercritical water gasification.

633 Table 3. Main results of modeling experimental extraction capacities of Ca and P by  
634 using the pseudo-second order kinetic equation.

635 Table 4. Formula, molar ratios Ca/P, and solubility constants of various Ca phosphates  
636 (adapted from Valsami-Jones (2001)).

637

638 **Figure captions**

639 Figure 1. P fractions extracted from WAO residues: average values from duplicates.

640 Figure 2. P extraction efficiencies after 24 h of contact time as a function of the liquid to  
641 solid ratio (L/S) for different extractant solutions (experimental data, the dotted lines are  
642 there to facilitate interpretation).

643 Figure 3. P concentrations and pH values of the leachates after 24 h of contact time as a  
644 function of the liquid to solid ratio (L/S) when using 1 M citric acid and 1 M HCl as  
645 extractant solutions (experimental data, the dotted lines are there to facilitate  
646 interpretation).

647 Figure 4. Experimental Ca and P extraction capacities as a function of time for the two  
648 different extractant solutions: (A) 1 M HCl at L/S ratio 10 L/kg; (B) 1 M citric acid at  
649 L/S ratio 10 L/kg. Average values from duplicates, bars indicating the range min-max  
650 values. Continuous curves show the modelled capacities using the pseudo-second order  
651 kinetic equation.

652 Figure 5. Direct correlation between moles of Ca extracted and moles of P extracted  
653 from WAO residues during kinetic experiments performed with 1 M HCl and 1 M citric  
654 acid at the L/S ratio of 10 L/kg: average values from duplicates.

655

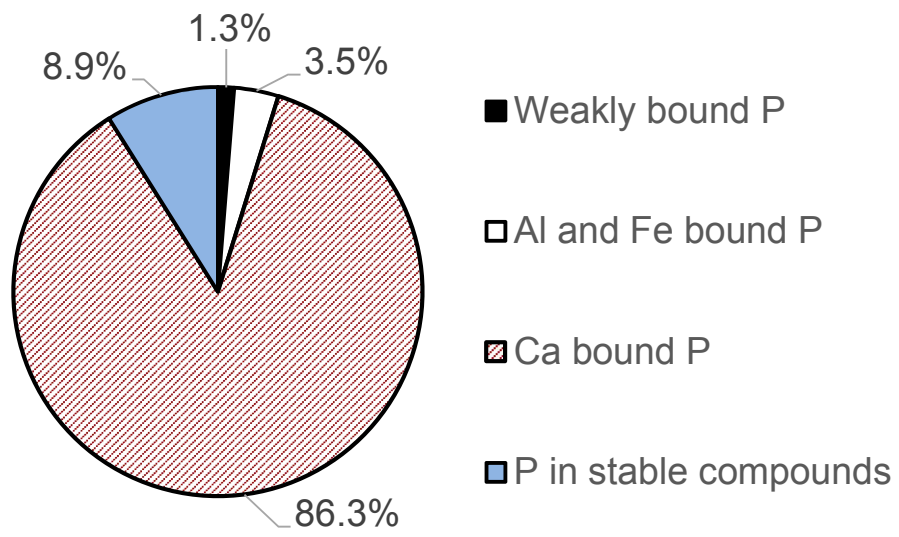


Figure 1. P fractions extracted from WAO residues: average values from duplicates.

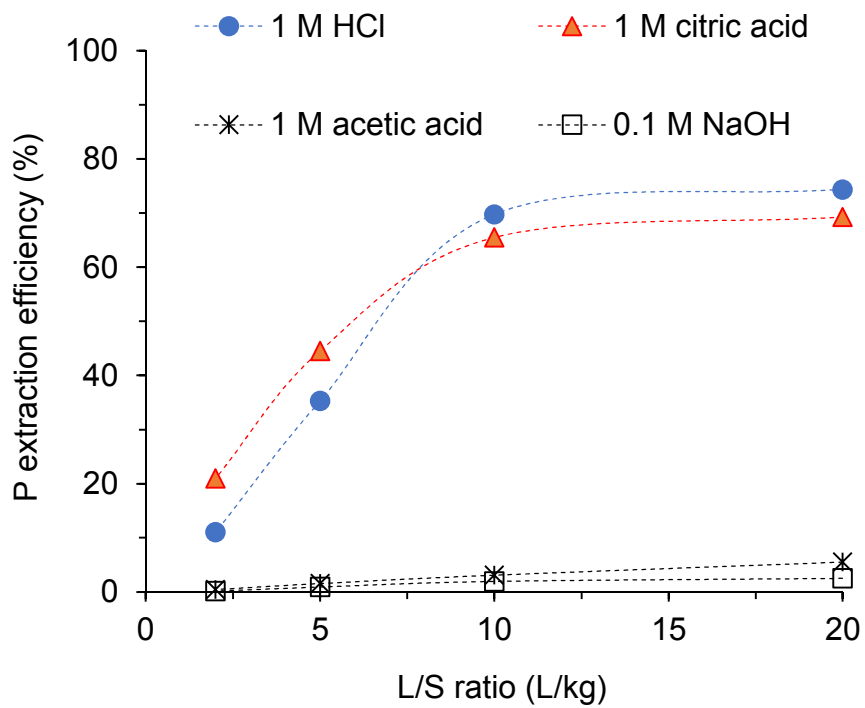


Figure 2. P extraction efficiencies after 24 h of contact time as a function of the liquid to solid ratio (L/S) for different extractant solutions (experimental data, the dotted lines are there to facilitate interpretation).

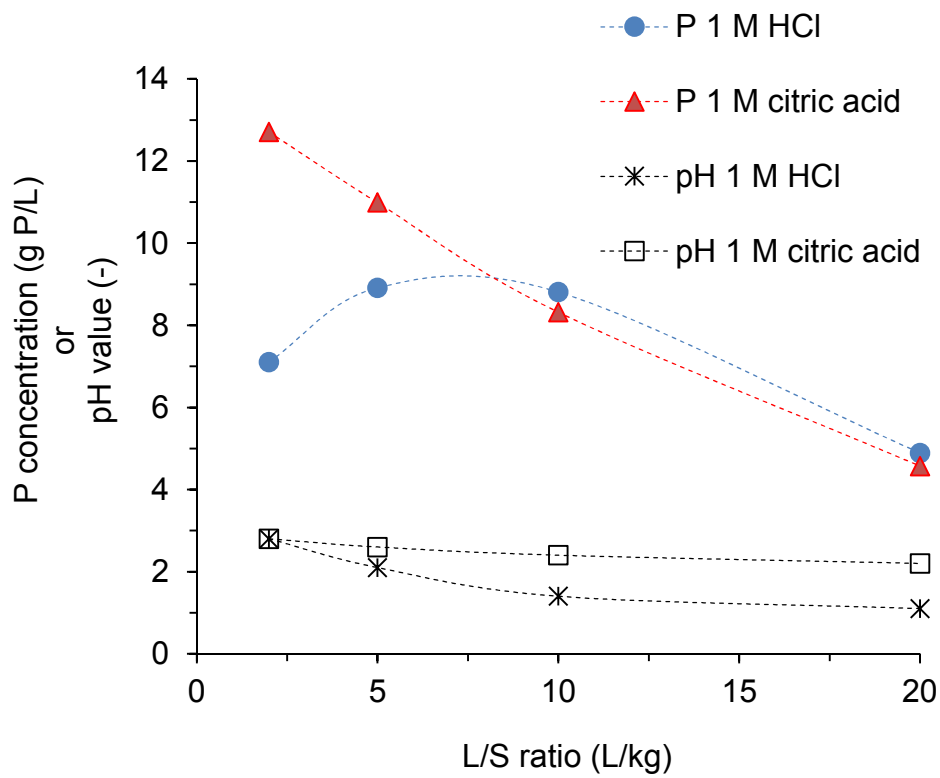


Figure 3. P concentrations and pH values of the leachates after 24 h of contact time as a function of the liquid to solid ratio (L/S) when using 1 M citric acid and 1 M HCl as extractant solutions (experimental data, the dotted lines are there to facilitate interpretation).

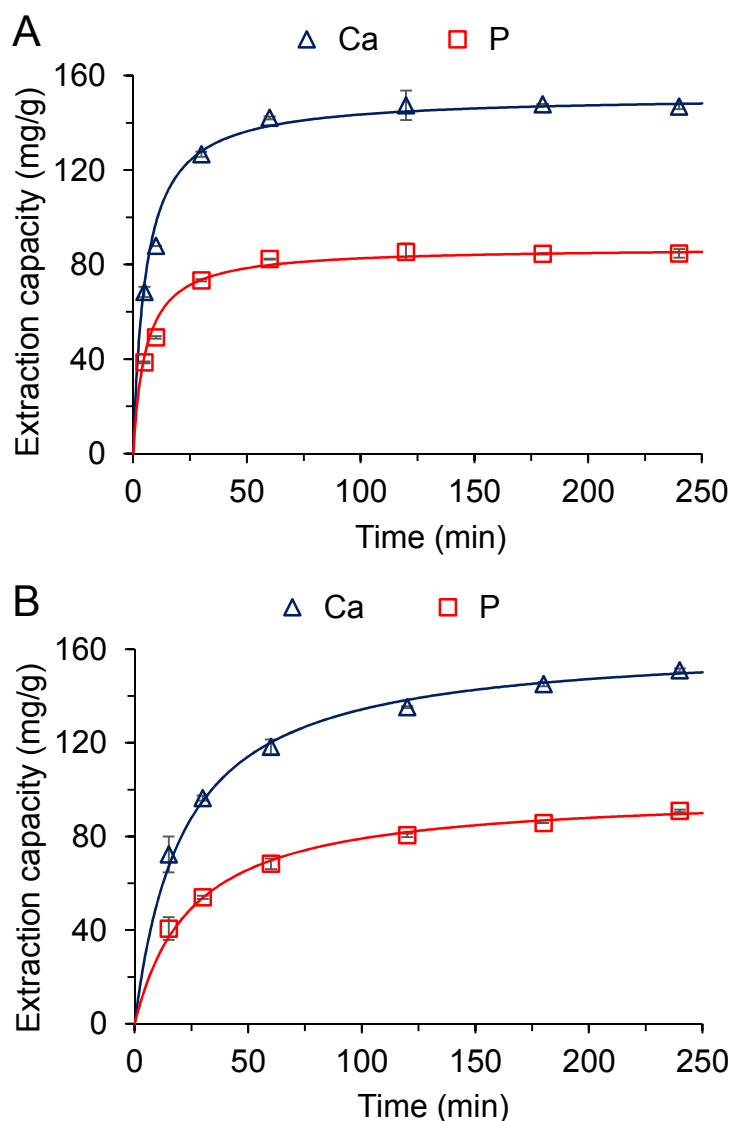


Figure 4. Experimental Ca and P extraction capacities as a function of time for the two different extractant solutions: (A) 1 M HCl at L/S ratio 10 L/kg; (B) 1 M citric acid at L/S ratio 10 L/kg. Average values from duplicates, bars indicating the range min-max values. Continuous curves show the modelled capacities using the pseudo-second order kinetic equation.

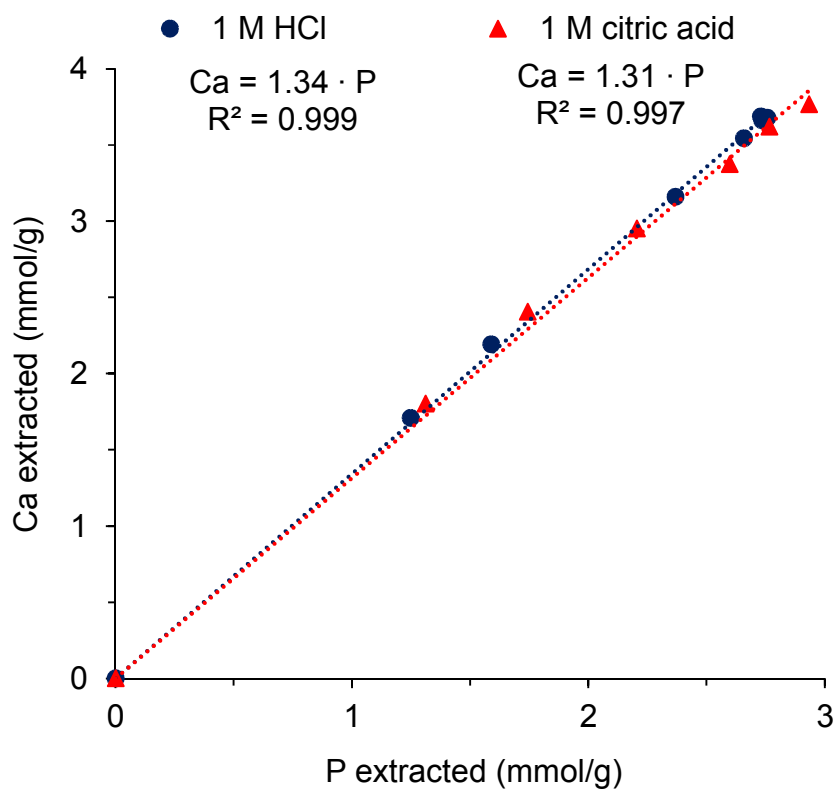


Figure 5. Direct correlation between moles of Ca extracted and moles of P extracted from WAO residues during kinetic experiments performed with 1 M HCl and 1 M citric acid at the L/S ratio of 10 L/kg: average values from duplicates.

Table 1. Element extraction capacities and efficiencies using 1 M citric acid and 1 M HCl after 24 h of contact time compared to *aqua regia* extraction capacities.

Element	<i>Aqua regia</i> extraction capacity <sup>a</sup> (mg/g)	1 M citric acid extraction at L/S ratio 10 L/kg		1 M HCl extraction at L/S ratio 10 L/kg	
		Capacity (mg/g)	Efficiency <sup>b</sup> (%)	Capacity (mg/g)	Efficiency <sup>b</sup> (%)
Al	19.8 ± 0.2	3.99	20	4.79	24
Ba	1.2 ± < 0.1	0.46	38	0.047	4
Ca	170 ± 2	132	78	149	88
Cd	0.016 ± 0.001	0.0032	20	0.0028	18
Co	0.012 ± < 0.001	0.0028	23	0.0024	20
Cr	0.14 ± < 0.01	0.026	19	0.027	19
Cu	2.5 ± 0.1	1.3	52	0.74	30
Fe	150 ± 1	42.0	28	31.9	21
K	3.0 ± 0.2	1.5	50	0.92	31
Mg	22.9 ± 0.1	11.3	49	12.6	55
Mn	0.44 ± < 0.01	0.26	59	0.16	36
Ni	0.066 ± 0.001	0.0095	14	0.011	17
P	132 ± 1	86.4	65	92.0	70
Pb	0.20 ± < 0.01	0.020	10	0.057	28
Se	0.066 ± 0.014	0.023	35	0.012	18
Si	0.272 ± 0.058	3.17	1160	2.64	970
V	0.015 ± 0.001	0.0075	50	0.0039	26
Zn	2.08 ± 0.02	1.09	52	0.774	37

<sup>a</sup>Average values ± standard deviation from duplicate experiments.

<sup>b</sup>Compared to *aqua regia* extraction.

Table 2. Main results of recent studies that have investigated P extraction from solid residues derived from thermal treatments of SS: ISS = incineration SS; PSS = pyrolysis SS; GSS = gasification SS; HTC = hydrothermal carbonization; SCWO = supercritical water oxidation; SCWG = supercritical water gasification.

Study	Residue tested		Optimum parameters and main results of P extraction				
	Type of residue	Process temperature and pressure	P content (g/kg)	Extractant solution	L/S ratio (L/kg)	Reaction time (h)	P extraction efficiency (%)
Stark et al., 2006	SCWO residue	> 374 °C, > 22 MPa	27-80	0.1 M HCl	50	2	80-100
Franz, 2008	ISS ash	830-850 °C	92	1.4 M H <sub>2</sub> SO <sub>4</sub>	2	0.167	90
Biswas et al., 2009	ISS ash	N.A.	88	0.1 M HCl or 0.05 M H <sub>2</sub> SO <sub>4</sub>	150	4	~ 100
Donatello et al., 2010	ISS ash	800-900 °C	54-76	0.5 M H <sub>2</sub> SO <sub>4</sub>	20	2	91
Petzet et al., 2012	ISS ash	N.A.	79-110	1 M NaOH <sup>a</sup>	10	24	70-77
Xu et al., 2012	ISS ash	850 °C	66-119	0.5 M HCl	50	2	95
Ottosen et al., 2013	ISS ash	850	70-99	0.19 M H <sub>2</sub> SO <sub>4</sub>	20	2	~ 100
Acelas et al., 2014	SCWG residue	400 °C, 24.6 MPa	83	pH 2 <sup>b</sup>	1000	8	84
		500 °C, 37.0 MPa	87				86
		600 °C, 49.6 MPa	94				95
Atienza–Martínez et al., 2014	ISS ash	600 °C	78	0.06 M oxalic acid	150	2	93
		750 °C	79				98
		900 °C	81				96
Huang and Tang, 2015	PSS char	250-600 °C	40-100	0.25 M NaOH + 0.05 M EDTA	20	16	40-65
	HTC char	225 °C	70-80				50-55
Kleemann et al., 2017	ISS ash	850-950 °C	72-75	0.6 M H <sub>2</sub> SO <sub>4</sub>	10	0.5	88-90
	PSS char	850 °C	56	0.8 M H <sub>2</sub> SO <sub>4</sub>			89
Gorazda et al., 2018	GSS char	800-1000 °C	87.6	2.7 M HNO <sub>3</sub>	~ 2.5	2	82
This study	WAO residue	274 °C, 4.5 MPa	132	1 M citric acid	10	2	61
				1 M HCl		1	62

<sup>a</sup> After acid pretreatment; <sup>b</sup> Continuously controlled by addition of oxalic acid.

Table 3. Main results of modeling experimental extraction capacities of Ca and P by using the pseudo-second order kinetic equation.

Element	Extractant (L/S = 10)	Main results of the pseudo-second order model		
		R <sup>2</sup>	q <sub>e</sub> <sup>a</sup> (mg/g)	k <sub>2</sub> <sup>a</sup> (g/(mg · min))
Ca	1 M HCl	0.999	151 ± 1	0.00120 ± 0.00022
P	1 M HCl	0.999	87.3 ± 0.7	0.00206 ± 0.00046
Ca	1 M citric acid	0.999	163 ± 1	0.000288 ± 0.000022
P	1 M citric acid	0.999	99.0 ± 1.1	0.000402 ± 0.000036

<sup>a</sup> Estimate parameters ± standard errors.

Table 4. Formula, molar ratios Ca/P, and solubility constants of various Ca phosphates (adapted from Valsami-Jones, 2001).

Name	Formula	Molar ratio Ca/P	Solubility constant (mol/L)
Dicalcium phosphate dihydrate (DCPD)	$\text{CaHPO}_4 \bullet 2\text{H}_2\text{O}$	1	$2.49 \cdot 10^{-7}$
Dicalcium phosphate anhydrous (DCPA)	$\text{CaHPO}_4$	1	$1.26 \cdot 10^{-7}$
Octacalcium phosphate (OCP)	$\text{Ca}_8\text{H}(\text{PO}_4)_6 \bullet 2,5 \text{H}_2\text{O}$	1.33	$1.25 \cdot 10^{-47}$
Tricalcium phosphate (TCP)	$\text{Ca}_3(\text{PO}_4)_2$	1.5	$1.20 \cdot 10^{-29}$
Hydroxyapatite (HAP)	$\text{Ca}_5(\text{PO}_4)_3\text{OH}$	1.67	$4.7 \cdot 10^{-59}$
Amorphous calcium phosphates (ACP)	variable	1-1.5	variable